Research in Pharmaceutical Sciences, June 2026; 21(3): 386-402
Received: 05-04-2025
Peer Reviewed: 07-05-2025
Revised: 02-06-2025
Accepted: 28-06-2025
Published: 10-05-2026

School of Pharmacy & Pharmaceutical Sciences
Isfahan University of Medical Sciences

Original Article

Synergistic cytotoxicity of recombinant IGFBP-3 and cisplatin in HPV18-positive HeLa cells *via* NF-κB inflammatory modulation

Hourolein Arab[1], Mohammad Shokrzadeh[2,*], Tahoora Mousavi[3], and Mohammad Reza Mofid[1,4,*]

[1]Department of Clinical Biochemistry, School of Pharmacy and Pharmaceutical Sciences, Isfahan University of Medical Sciences, Isfahan, Iran. [2]Department of Toxicology and Pharmacology, Faculty of Pharmacy, Mazandaran University of Medical Sciences, Sari, Iran. [3]Molecular and Cell Biology Research Center, Hemoglobinopathy Institute, Faculty of Medicine, Mazandaran University of Medical Sciences, Sari, Iran. [4]Bioinformatics Research Center, School of Pharmacy and Pharmaceutical Sciences, Isfahan University of Medical Sciences, Isfahan, Iran.

Abstract

Background and purpose: Insulin-like growth factor-binding protein-3 (IGFBP-3), a tumor suppressor and inhibitor of nuclear factor kappa B (NF-κB), has emerged as a promising candidate for therapeutic application across diverse pathological conditions. Given NF-κB's role in cervical cancer development and cisplatin resistance, this study examines the effects of recombinant human IGFBP-3 (rhIGFBP-3), alone and in combination with cisplatin, on NF-κB levels, inflammatory modulation, and apoptotic response in HeLa cells, and investigates whether rhIGFBP-3 can reduce the cisplatin dose.

Experimental approach: The impact of rhIGFBP-3, alone and in combination with cisplatin, on HeLa cells' viability was evaluated by assessing cell viability (MTT assay); apoptosis (cell cycle analysis, TUNEL, annexin V/PI staining, Bax/Bcl-2 ratio, caspase activity); and NF-κB p65 levels (western blot). Gene expression of inflammatory cytokines and enzymes (IL-6, IL-8, COX-2, iNOS) was analyzed by RT-PCR.

Findings/Results: Cisplatin and rhIGFBP-3 inhibited HeLa cell growth in a concentration-dependent manner (IC_{50} = 6.06 µg/mL and 1.12 µg/mL, respectively). Their combination exhibited synergistic cytotoxicity (combination index < 1), allowing ~2.1-fold reductions in concentration to 2.53 µg/mL cisplatin and 0.46 µg/mL rhIGFBP-3 for 45% growth inhibition. Compared to monotherapy, the combination significantly enhanced apoptosis and DNA fragmentation, sub-G1 accumulation, caspase-8/9/3/7 activation, and BAX/BCL-2 ratio. It also considerably reduced NF-κB p65 and inflammatory markers in comparison with cisplatin alone.

Conclusion and implications: Our study demonstrated that rhIGFBP-3 enhanced cisplatin efficacy by promoting apoptosis and attenuating inflammation, highlighting its potential as both a cisplatin adjuvant and a monotherapy in HeLa cells.

Keywords: Apoptosis, Cervical cancer; Cisplatin; IGFBP-3; Inflammation; NF-κB.

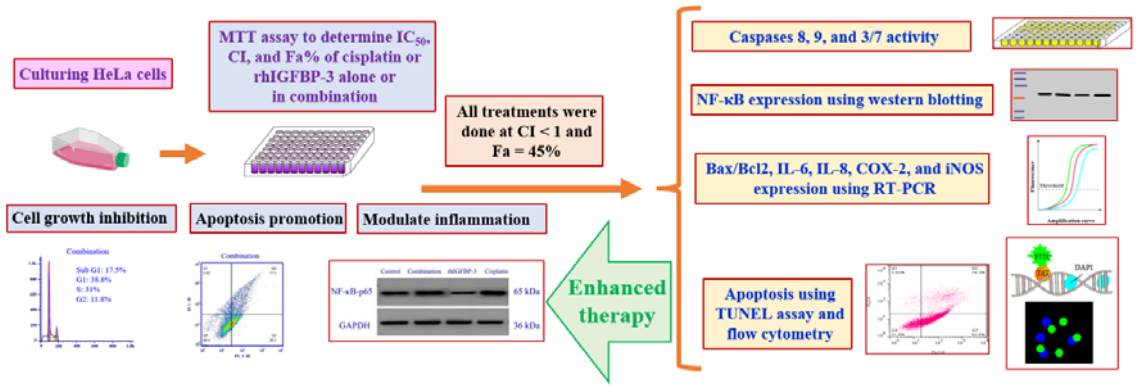

*Corresponding authors:
M.R. Mofid, Tel: +98-3137927047, Fax: +98-3136680011
Email: mofid@pharm.mui.ac.ir
M. Shokrzadeh, Tel: +98-9111263448, Fax: +98-1513542472
Email: mshokrzadeh@mazums.ac.ir

Access this article online

Website: http://rps.mui.ac.ir

DOI: 10.4103/RPS.RPS_62_25

INTRODUCTION

Cervical cancer (CC) remains a critical health concern worldwide, as it is still one of the most frequently diagnosed cancers in women, despite advances in screening, prevention, and early detection of high-risk human papillomavirus (HPV), and treatment options such as radiation, chemotherapy, and surgery (1). Unfortunately, the adverse effects of existing treatments continue to affect patients' quality of life negatively. Therefore, this draws attention to the pressing need for more potent and less detrimental treatment methods (2).

Cisplatin is commonly used alone or in combination with other treatments for CC. However, severe side effects, including gastrointestinal, neurological, hematologic, and ototoxicity, limit its use and complicate disease management (3). Furthermore, cisplatin's therapeutic impact is often diminished, particularly in advanced cervical malignancies in which treatment resistance has developed. A complex interaction of factors contributes to the progression of CC and reduces chemotherapy efficacy, although the underlying molecular processes are not fully understood (4).

It is well established that CC is a chronic inflammatory disease influenced by a variety of factors (5-7). Several studies have identified nuclear factor kappa B (NF-κB), an inflammatory transcription factor, as a critical player in the inflammation associated with CC. NF-κB is a key mediator of signaling pathways that regulate genes involved in carcinogenesis and chemotherapy resistance, particularly with platinum-based drugs such as cisplatin (8,9). Both cisplatin and HPV E6 and E7 oncogenes enhance NF-κB activation. These oncogenes drive cervical cells toward cancer by persistently activating the NF-κB inflammatory signaling pathway. Cisplatin further contributes to chemotherapy resistance and exacerbates the challenges in treating CC (10-12). Targeting NF-κB has emerged as a promising strategy to enhance anticancer therapies by inhibiting tumor cell survival and resistance. However, current NF-κB inhibitors may have off-target effects; therefore, there is a need to identify novel therapeutic compounds (13).

Insulin-like growth factor-binding protein-3 (IGFBP-3) is the most prevalent member of the IGFBP family and has demonstrated anti-tumor activity in various cancers, including those of the stomach, liver, pancreas, cervix, breast, lung, and prostate, particularly when its expression is upregulated or combined with anticancer treatments (14-20). Furthermore, its interaction with transmembrane protein 219 (TMEM219) has been shown to induce caspases 8, 7, and 3, leading to the degradation of the NF-κB p65 protein and, consequently, the loss of NF-κB function (21). Inhibition of NF-κB *via* IGFBP-3 is beneficial in conditions such as atherosclerosis, rheumatoid arthritis, asthma, and liver disease (22-25).

To date, studies have primarily focused on IGFBP-3's anti-tumor activities in various cancers or its anti-inflammatory role in inflammatory diseases. Surprisingly, limited attention has been given to the effects of exogenous IGFBP-3, both alone and in combination with cisplatin, on cancer-related inflammation in CC HeLa cells, or whether it promotes or suppresses tumorigenesis. Furthermore, its impact on the NF-κB signaling pathway in CC remains unexplored. This study addressed these gaps by evaluating IGFBP-3's effects, alone and in combination with cisplatin, on growth inhibition, apoptosis, cell cycle regulation, and NF-κB-mediated inflammatory signaling in CC.

MATERIALS AND METHODS

Chemicals and reagents

Dulbecco's modified Eagle medium with high glucose (DMEM-HG) was commercially sourced from Gibco (Thermo Fisher Scientific, Waltham, MA, USA). rhIGFBP-3 was provided by Bioscience (Canada), and cisplatin was provided by Sobhan Daru Pharmaceutical Company, Iran. Horseradish peroxidase (HRP)-conjugated secondary antibody was purchased from Santa Cruz Biotechnology, Inc (Dallas, TX, USA). Anti-NF-κB p65, anti-glyceraldehyde-3-phosphate dehydrogenase (GAPDH) primary antibodies, and other essential reagents for western blotting were procured from Cell Signaling Technology and Thermo Scientific (USA). Terminal deoxynucleotidyl transferase dUTP nick end labeling (TUNEL), annexin V-fluorescein isothiocyanate/propidium iodide (Annexin V-FITC/PI), and caspase activity assay kits were supplied by Elabscience (Houston, TX, USA).

Molecular materials were purchased from Pars Toos Company, Iran.

Cell growth and experimentation

The human cervical adenocarcinoma cell line (HeLa, HPV18-positive) was sourced from the Iran Stem Cell Technology Research Center. Incubation conditions for the cells were as follows: DMEM-HG, 37 °C, 5% CO_2, 10% fetal bovine serum (FBS), and 1% penicillin-streptomycin. Once the cells reached 70-80% confluence, they were detached from T25 flasks using a trypsin-EDTA solution for 4 min. Viable cells were counted using trypan blue staining. Subsequently, 2,500 cells were dispensed into individual wells of 96-well plates and treated with either rhIGFBP-3 or cisplatin for 48 h, across a range of concentrations (0 to 25 µg/mL for cisplatin and 0 to 4 µg/mL for rhIGFBP-3).

MTT cell viability assay

The cytotoxic effects of cisplatin and rhIGFBP-3 on HeLa cells were assessed by means of a colorimetric assay relying on the reduction of the yellow tetrazolium dye, which produces a purple coloration in the 3-(4,5-dimethylthiazol-2-yl)-2,5-diphenyltetrazolium bromide (MTT) assay. As an initial step, HeLa cells were exposed to a predefined concentration of cisplatin and rhIGFBP-3 for 48 h. Subsequently, an MTT solution (0.5 mg/µL) was added, and incubation was continued for approximately 3.5 h. After removal of the MTT-containing medium, 200 µL of dimethyl sulfoxide (DMSO) was added to dissolve the resulting purple formazan crystals, and the 96-well culture plate was agitated on a shaker for 20 min. A Chromate-4300 microplate spectrophotometer (Awareness Technology Inc., Palm City, FL, USA) recorded absorbance at 570 nm. Each experimental condition was run in triplicate, and the entire procedure was executed three times under identical conditions. The following equation was used to calculate the percentage of cell survival:

$$Cell\ survival\ (\%)$$

$$\frac{OD\ of\ test\ sample\ -\ OD\ of\ blank}{OD\ of\ control\ -\ OD\ of\ blank} \times 100$$

where OD stands for optical density.

Quantification of the combination index between cisplatin and rhIGFBP-3 co-treatment

The combinatory effect of cisplatin and rhIGFBP-3 co-treatment was evaluated using the fixed-ratio methodology developed by Chou and Talalay (26). The fixed ratio of 5.5:1 was calculated by dividing the half-maximal inhibitory concentration (IC_{50}) of cisplatin (6.06 µg/mL) by that of rhIGFBP-3 (1.12 µg/mL), as determined individually using the MTT assay. Based on this ratio, combination concentrations were prepared by serially diluting cisplatin across a range of 0.5-8 µg/mL, with corresponding rhIGFBP-3 concentrations adjusted proportionally (i.e., 0.09-1.45 µg/mL) to maintain the 5.5:1 ratio throughout. HeLa cells were subjected to these combinations for 48 h, after which cell viability was evaluated through the MTT assay. Combination index (CI) values were derived by employing CompuSyn software. The CI was determined for each affected fraction (fa), where fa is defined as the percentage of inhibition divided by 100. A CI value greater than 1 suggests antagonism, values lower than 1 signify synergism, and a value equal to 1 reflects an additive effect.

Annexin V/PI cytometric analysis

As directed by the double staining kit, HeLa cells were marked using Annexin V and PI. Before treatment with specific concentrations of cisplatin and rhIGFBP-3 for 48 h, 3×10^5 HeLa cells were plated into wells and incubated overnight. Following this, the cells were rinsed with phosphate-buffered saline (PBS), released by incubation with trypsin-EDTA solution, and collected by centrifugation. Subsequently, the cells were rinsed once more at 4 °C with PBS (pH 7.4). Finally, after being washed with 1× annexin-binding buffer, the cells were gently reconstituted in 100 µL of buffer supplemented with 1 µL of PI and 5 µL of annexin V, followed by a 15-min incubation in the dark. Flow cytometry-derived data were processed using FlowJo 7.6.1 software to identify necrotic, late apoptotic, and early apoptotic cells.

Cell cycle profiling

The treatment and incubation of HeLa cells for cell cycle analysis were performed similarly to the previous experiment. Following treatment, harvested cells were washed with pre-chilled PBS and then fixed by incubation in 70% ice-cold ethanol at -20 °C for 30 min. After fixation, the cells underwent washing with PBS and were subsequently labeled with PI (50 µg/mL) and RNase A (100 µg/mL). The labeled cells were placed in a cell culture incubator for 30 min. Finally, a minimum of 10,000 cells per group were used to determine the distribution across various stages of the cell cycle *via* FlowJo 7.6.1 software (FlowJo LLC, Ashland, OR, USA).

DNA fragmentation method

The extent of DNA fragmentation in the treated cells was quantified *via* the TUNEL assay. In brief, after fixing the cells in 4% methanol-free paraformaldehyde, the cells were cleansed three times with PBS and kept at 4 °C, each wash lasting 30 min. Next, the terminal deoxynucleotidyl transferase equilibrium buffer was applied to each slide and incubated at 37 °C for 1 h. Upon completion of incubation, the slides were rinsed three times with PBS for 5 min each and then air-dried using absorbent paper. Subsequently, 4′,6-diamidino-2-phenylindole (DAPI) was administered, and the slides were incubated at 25 °C for approximately 5 min, followed by four additional PBS washes. Apoptotic nuclei were visualized as green fluorescence. Images were acquired *via* a digital camera connected to a fluorescence microscope, with excitation wavelengths between 450 and 500 nm and emission between 515 and 565 nm.

Western blot analysis

The treated cells were taken from the surface of the plate and lysed using radioimmunoprecipitation assay lysis buffer containing 0.5 mM phenylmethylsulfonyl fluoride, 0.5% protease inhibitor cocktail, and an ultrasonic probe in an ice bath to determine the total protein content using the Bradford method. Equal concentrations of protein per sample were electrophoretically separated on 12% sodium dodecyl-sulfate polyacrylamide gel electrophoresis (SDS-PAGE) and were then transferred to a polyvinylidene fluoride membrane. The membranes underwent overnight incubation at 4 °C with primary antibodies targeting NF-κB p65 (1:1000, #8242) and GAPDH (1:1000, #5174). Blocking was performed with 5% nonfat milk dissolved in tris-buffered saline supplemented with 0.1% tween 20 (TBST) for 2 h at 25 °C. Following three washes with TBST, the membranes received incubation treatment with an HRP-conjugated secondary antibody (1:5000, sc-2357) for 2 h at 25 °C. After three washes with TBST, the blots were visualized on X-ray film using an enhanced chemiluminescence kit. ImageJ software was used to quantify band intensities, which were then normalized to GAPDH.

Procedure for caspase 8, 9, and 3/7 activity detection

Based on the mentioned kits, at least 300,000 cells were cultivated in each well of 6-well plates until they reached the desired confluence and were subjected to specific treatment. Then, the cells were extracted, centrifuged, and finally lysed in cold buffer. To the cytolysis samples, a reaction buffer was added for the final reaction, followed by the addition of specific substrates for each caspase. The mixtures were incubated at 37 °C for 2 h, and absorbance readings at 405 nm were used to quantify enzyme activity. Each of the experiments was done three times, and the enzyme activity was calculated from a previously established p-nitroaniline standard curve.

Quantitative real-time polymerase chain reaction

Following the procedure, total RNA was collected from all group cells using a protocol provided by the Pars Toos Company (Iran). The RNA concentration and purity of the extracts were quantitatively assessed *via* a Nanodrop spectrophotometer and qualitatively confirmed by agarose gel electrophoresis. The Pars Toos Easy complementary DNA (cDNA) synthesis kit was utilized for cDNA synthesis. Primer sequences for the reference and target genes were developed utilizing gene sequences obtained from the National Center for Biotechnology Information (NCBI) database, using Primer3 software. The sequences were further validated using the NCBI Basic Local Alignment Search Tool software (Table 1).

Table 1. Assembled mRNA sequences for target genes.

Gene name	Sequence (5' > 3')	Length
IL-8	Forward: GAGAGTGATTGAGAGTGGACCAC Reverse: CACAACCCTCTGCACCCAGTTT	115
iNOS	Forward: GCTCTACACCTCCAATGTGACC Reverse: CTGCCGAGATTTGAGCCTCATG	134
COX-2	Forward: CGGTGAAACTCTGGCTAGACAG Reverse: GCAAACCGTAGATGCTCAGGGA	110
IL-6	Forward: AGACAGCCACTCACCTCTTCAG Reverse: TTCTGCCAGTGCCTCTTTGCTG	133
BAX	Forward: AAGAAGCTGAGCGAGTGTCT Reverse: TGCCGTCAGAAAACATGTCAG	142
BCL2	Forward: AGAGTTGCTTTACGTGGCCT Reverse: AGCACCACTGCATTTCAGGA	116
GAPDH	Forward: GGTGGTCTCCTCTGACTTCAACA Reverse: GTTGCTGTAGCCAAATTCGTTGT	127

Bcl-2, B-cell lymphoma 2; BAX, Bcl-2-associated X protein; IL, interleukin; COX, cyclooxygenase; iNOS, inducible nitric oxide synthase.

To determine the relative mRNA levels of the target genes, quantitative real-time polymerase chain reaction (qRT-PCR) analysis was performed using the StepOne Real-Time PCR System (Applied Biosystems, Foster City, CA, USA) and Kiagene 2X SYBR Green PCR master mix. The control gene, GAPDH, was employed. The amplification process started with an initial denaturation at 95 °C for 2 min (1 cycle), succeeded by 40 cycles of denaturation at 95 °C for 5 s, annealing at optimized temperatures [GAPDH: 60 °C; B-cell lymphoma 2 (BCL-2): 55 °C; BCL-2-associated X protein (BAX): 53 °C; cyclooxygenase-2 (COX-2): 57 °C; interleukin-6 (IL-6): 62 °C; IL-8: 63 °C; inducible nitric oxide synthase (iNOS): 52 °C] for 20 s, followed by an extension at 72 °C for 25 s, concluding with a final extension at 72 °C for 1 min (1 cycle). The relative transcript expression levels were estimated using the $2^{-\Delta\Delta CT}$ formula.

Statistical analyses

GraphPad Prism 10.5.0 (774) (version 10.5.0, build 774; GraphPad Software, San Diego, CA, USA) was selected to statistically analyze data from three replicates in two additional separate assessments, presenting the results as mean ± SD. Evaluation of the data normality was performed using the Shapiro-Wilk test, and the difference between groups relative to the control group was assessed using a one-way analysis of variance (ANOVA) test, followed by Tukey's and Dunnett's post-hoc tests. P-values < 0.05 were considered statistically significant.

RESULTS

Growth-restraining effects of cisplatin and rhIGFBP-3, individually and in combination

Cytotoxic effects of cisplatin and rhIGFBP-3, either alone or in combination, were evaluated in HeLa cells after 48 h using the MTT assay (Fig. 1A). A statistically significant cytotoxic effect of cisplatin was observed starting at a concentration of 1.5 µg/mL. rhIGFBP-3 exhibited significant cytotoxic effects beginning at 0.5 µg/mL, with a marked concentration-dependent increase at higher concentrations. The IC_{50} values for cisplatin and rhIGFBP-3 were calculated to be 6.06 ± 0.26 µg/mL and 1.12 ± 0.034 µg/mL, respectively. The combined inhibitory effects of cisplatin and rhIGFBP-3 were assessed using various concentration combinations, with the CI value being determined according to the method of Chou and Talalay, which employs the median-effect equation. The IC_{50} for the combined treatment group was calculated to be 3.63 ± 0.28 µg/mL, calculated from cell survival data as described in the MTT cell viability assay section, indicating that rhIGFBP-3 enhances the

cytotoxic effect of cisplatin. Phase-contrast microscopy revealed marked morphological changes in HeLa cells following treatment with varying concentrations of the rhIGFBP-3 and cisplatin combination (Fig. 1B). Control cells maintained high density and normal morphology. However, as the concentration of the combined treatment increased (from 0.09 + 0.5 µg/mL to 1.45 + 8 µg/mL), a substantial reduction in the proportion of viable cells was observed. This was accompanied by significant morphological alterations, including cell shrinkage, rounding, and detachment, characteristic of apoptosis, along with a concentration-dependent reduction in cell viability, as determined *via* the MTT assay. However, CI values for fa levels above 50% exceeded 1, indicating an antagonistic effect between the two agents (Table 2, Fig. 2A and B). Conversely, at fa values below 50%, the dose reduction index (DRI) was favourable for both drugs, with DRI values greater than 1. The greatest cytotoxicity and the most advantageous dose reduction were observed for cisplatin at an fa of 45%, with a 2.13-fold dose reduction. Therefore, the combined treatment of cisplatin (2.53 µg/mL) and rhIGFBP-3 (0.46 µg/mL) was selected for further experimental evaluation (Table 2).

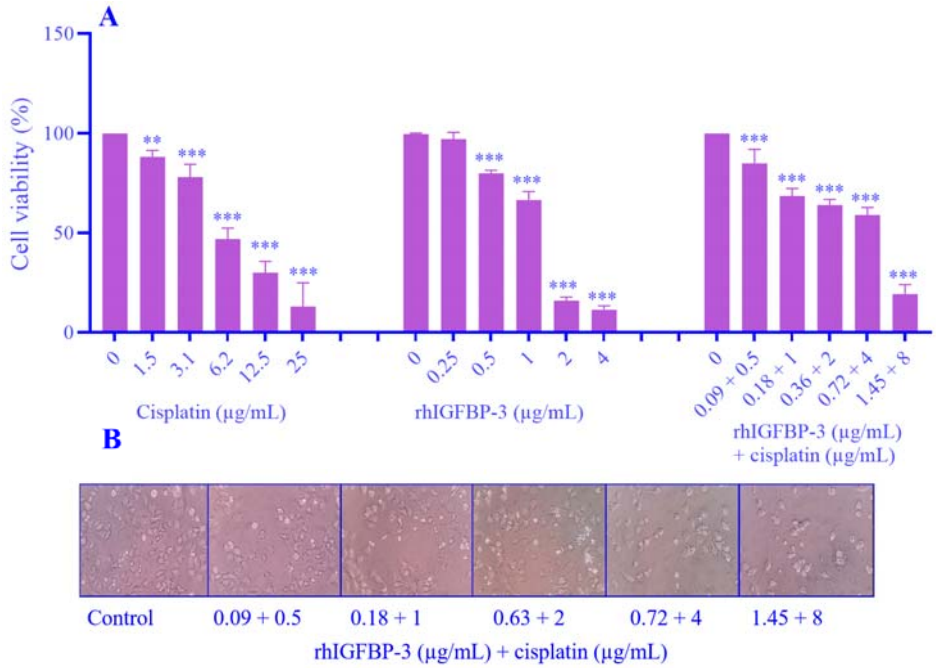

Fig. 1. Cytotoxic effects of cisplatin, rhIGFBP-3, and their combined treatment on HeLa cells after 48 h. (A) HeLa cell viability after 48-h treatment with cisplatin, rhIGFBP-3, and their combination. Data are expressed as mean ± SD; assays were performed in triplicate in three independent experiments (n = 9). $P < 0.05$, $^{**}P < 0.01$, $^{***}P < 0.001$ indicate significant differences in comparison with the control group. (B) Phase-contrast microscopy images of cells treated with combinations of rhIGFBP-3 and cisplatin at different concentrations reveal the percentage of viable cells and morphological changes observed after 48 h. rhIGFBP, Recombinant human insulin-like growth factor-binding protein 3.

Table 2. Combination and DRIs for cisplatin and rhIGFBP-3.

Fraction affected (%)	Cisplatin (µg/mL)	rhIGFBP3 (µg/mL)	CI value	DRI (cisplatin)	DRI (rhIGFBP3)
40	4.803	0.864	0.869	2.311	2.286
45	5.404	0.987	0.935	2.131	2.142
50	6.066	1.125	1.005	1.969	2.010
75	11.418	2.304	1.487	1.277	1.418
90	21.491	4.719	2.206	0.828	1

rhIGFBP, Recombinant human insulin-like growth factor-binding protein 3; DRI, dose reduction indices.

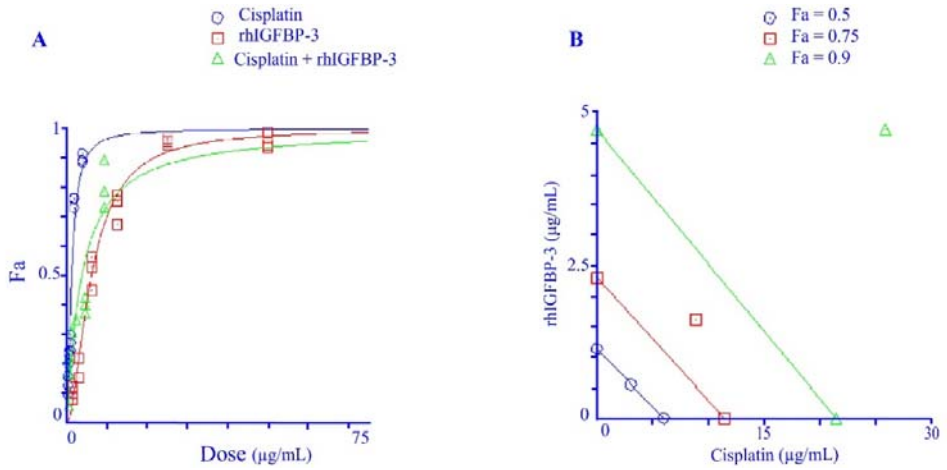

Fig. 2. Effect of the combination of cisplatin and rhIGFBP-3 on HeLa cells. (A) Concentration-effect curves for cisplatin, rhIGFBP-3, and their combination, reflecting the effects of fa at levels of 0.5, 0.7, and 0.9 for each treatment. (B) Isobologram demonstrating the combined effects of cisplatin and rhIGFBP-3 at different concentrations. rhIGFBP, Recombinant human insulin-like growth factor-binding protein 3.

Apoptotic effects of cisplatin and rhIGFBP-3, both alone and in combination

The inhibitory mechanism of cisplatin and rhIGFBP-3 on HeLa cell proliferation was assessed by quantifying apoptotic and necrotic cell populations using annexin V-FITC/PI dual-labeling. Based on our previous calculations, cells were treated in four groups for 48 h as follows: cisplatin (2.53 μg/mL), rhIGFBP-3 (0.46 μg/mL), a combination group (2.53 μg/mL cisplatin + 0.46 μg/mL rhIGFBP-3), and an untreated control group. As demonstrated in Fig. 3A and B, the proportions of apoptotic cells in the cisplatin-alone, rhIGFBP-3-alone, and combination treatment groups were markedly elevated compared to the untreated control group, with values of 32.3 ± 1.06%, 22.99 ± 0.88%, 45.72 ± 1.05%, and 0.87 ± 0.58%, respectively. The combination group induced a significantly greater apoptotic response than either cisplatin or rhIGFBP-3 alone.

DNA fragmentation effects of cisplatin and rhIGFBP3, both alone and in combination

Following treatment with the predetermined duration and concentration, DNA fragmentation in HeLa cells was assessed using the TUNEL method. Figure 4A shows fluorescent images of HeLa cells containing DNA fragments. The overall number of TUNEL-positive cells rose appreciably in the treated groups compared to the untreated control group. The number of TUNEL-positive cells was significantly elevated following the combination treatment, compared to either single-treatment group. The results indicate that the combined treatment leads to a marked elevation in apoptosis in HeLa cells relative to either single-agent treatment or the control condition (Fig. 4B).

Effects of cisplatin and rhIGFBP-3 and their combination on cell cycle arrest

We used PI labeling and flow cytometry to examine the effects of cisplatin and rhIGFBP-3, either individually or in combination, on cell cycle distribution 48 h after treatment. Treatment with cisplatin led to an evident increase in the sub-G1 population, indicating elevated levels of apoptosis, along with a marked decrease in the number of cells in the G1 phase compared to the control group. However, Fig. 5A and B did not show significant changes in the populations of cells in the G2/M and S phases. The sub-G1 population following rhIGFBP-3 treatment remained low compared to both the cisplatin and control groups, although the treatment induced a notable accumulation of cells in the G1 phase (60.16 ± 1.04%), suggesting G1 phase arrest. Combined treatment with cisplatin and rhIGFBP-3 significantly increased the sub-G1 population compared to the control group (17.16 ± 1.04% *vs.* 0.75 ± 0.25%), indicating a rise in apoptotic cells. In this group, the G1 phase population was significantly reduced, and the distributions in S and G1 phases remained unchanged.

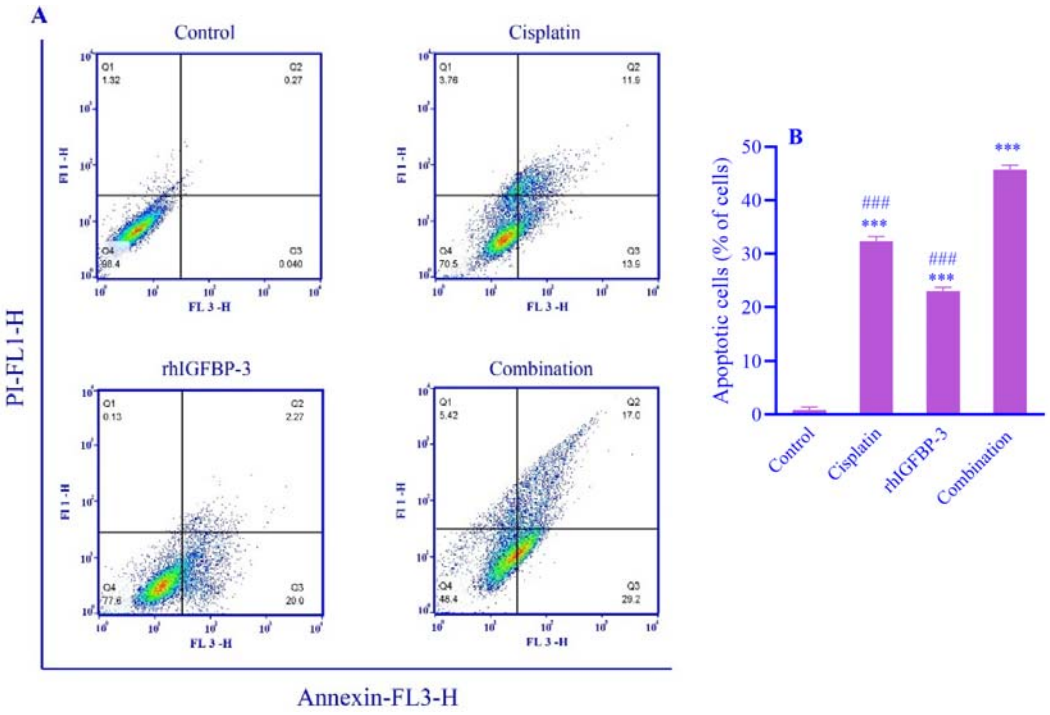

Fig. 3. Apoptosis induced by cisplatin, rhIGFBP-3, and their combination in HeLa cells. The proportion of stained HeLa cells was evaluated and compared with that of untreated control cells. (A) Flow cytometric plots indicating Q4 for live cells (annexin V^-/PI^-), Q3 for early apoptotic cells (annexin V^+/PI^-), Q2 for late apoptotic cells (annexin V^+/PI^+), and Q1 for necrotic cells (annexin V^-/PI^+). (B) The quantitative proportion of apoptotic cells; the data are expressed as mean ± SD of three independent experiments, each performed in triplicate. ***$P \leq 0.001$ indicates significant differences in comparison with the control group, $^{\#\#\#\#}P \leq 0.001$ versus the combination. rhIGFBP, Recombinant human insulin-like growth factor-binding protein 3; PI, propidium iodide.

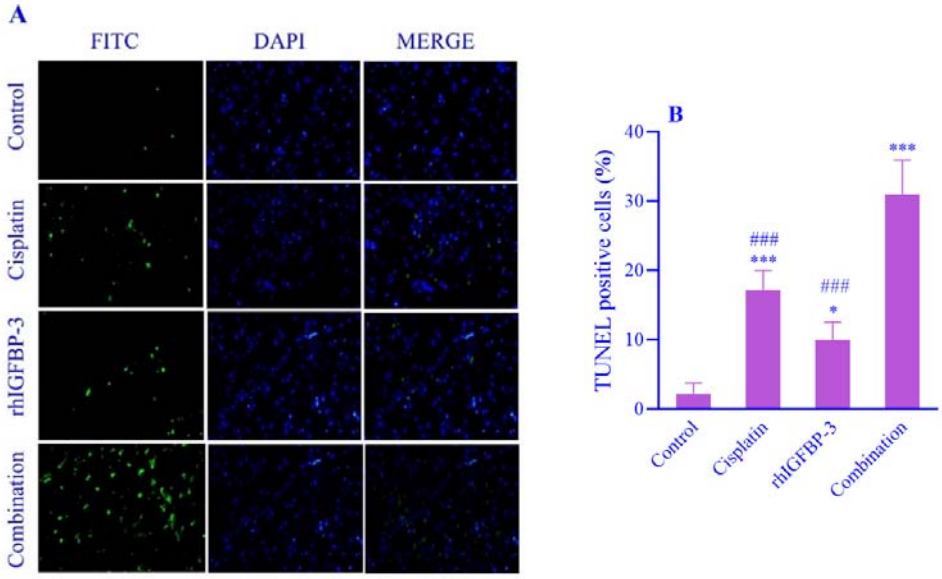

Fig. 4. DNA fragmentation induced by cisplatin, rhIGFBP-3, and their combination in HeLa cells after 48-h treatment. DNA fragmentation in treated HeLa cells was assessed using the TUNEL assay and compared to untreated control cells. (A) Fluorescent images of untreated and treated HeLa cells with FITC staining (green) to indicate apoptotic cells and DAPI (blue) to label all nuclei. The merged images show the ratio of apoptotic cells (green) to the total cell population (blue). (B) The bar graph represents DNA fragmentation and the number of apoptotic cells. The data are presented as mean ± SD from three independent experiments, each performed in triplicate. *$P < 0.05$ and ***$P \leq 0.001$ indicate significant differences in comparison with the control group, $^{\#\#\#\#}P \leq 0.001$ versus the combination. rhIGFBP, Recombinant human insulin-like growth factor-binding protein 3; FITC, fluorescein Isothiocyanate; DAPI, 4′,6-diamidino-2-phenylindole.

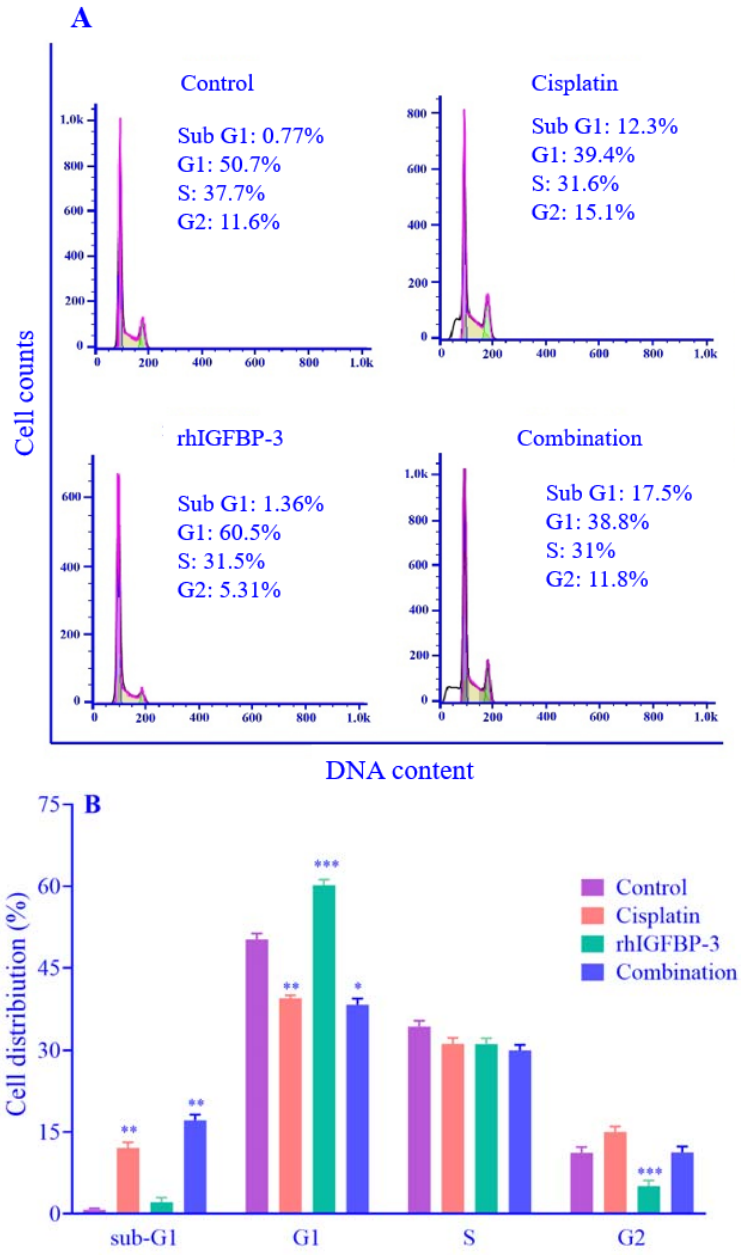

Fig. 5. Cell cycle distribution of HeLa cells after 48-h treatment with rhIGFBP-3, cisplatin, and their combination. (A) Histograms of cell cycle distribution indicate that the quantity of Sub-G1, G1, S, and G2 phases varies considerably in different treatments. (B) The bar graph presents the proportion of cells in every phase after treatment. Data are presented as mean ± SD from three independent experiments. *$P < 0.05$ and ***$P \leq 0.001$ indicate significant differences in comparison with the control group. rhIGFBP, Recombinant human insulin-like growth factor-binding protein 3.

Modulation of NF-κB p65 subunit expression by cisplatin, rhIGFBP-3, and their combination

We used the western blot method to evaluate NF-κB p65 protein levels following treatment with cisplatin, rhIGFBP-3, or their combination, as this protein is an essential signaling factor governing inflammation and cellular survival in HeLa cells. Figure 6A displays representative blots indicating NF-κB p65 and GAPDH levels. The results demonstrated a notable elevation in NF-κB p65

levels in cisplatin-treated cells compared to the untreated control group, confirming that cisplatin upregulates the protein. In contrast, rhIGFBP-3 alone significantly reduced NF-κB p65 levels. Notably, co-treatment with both agents contributed to a substantial decline in NF-κB p65 levels relative to cisplatin administration alone, although the levels remained significantly higher than those in the rhIGFBP-3 and control groups (Fig. 6B). Overall, these findings suggest that rhIGFBP-3 reduces NF-κB p65 subunit levels, while cisplatin enhances them.

Impact of cisplatin and rhIGFBP-3, alone and combined, on caspase activity

Following the observation of cell death in treated HeLa cells, we investigated whether these treatments could stimulate the activity of caspases 8, 9, and 3/7, which are the main catalysts of programmed cell death. The results confirmed that, compared to untreated cells, both cisplatin and rhIGFBP-3 individually induced a marked increase in caspase activity. Moreover, their combination significantly enhanced this effect, both relative to the control group and the individual treatment (Fig. 7A-C).

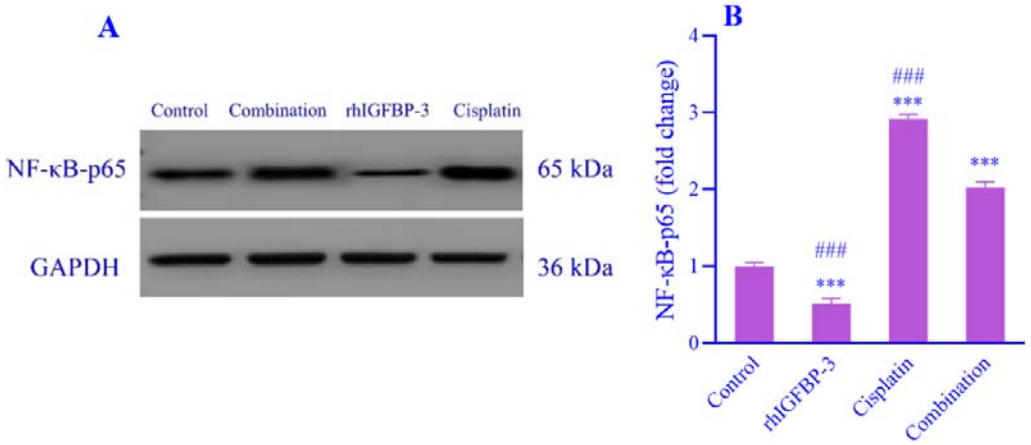

Fig. 6. Impact of cisplatin, rhIGFBP-3, and their combination on NF-κB p65 protein levels in HeLa cells. (A) Immunoblot images portray NF-κB p65 protein levels adjusted using GAPDH as an internal reference. (B) The bar graph expresses the mean fold change in NF-κB p65 expression ± SD, obtained from two experiments. ***$P \leq 0.001$ indicates significant differences in comparison with the control group, $^{\#\#\#}P \leq 0.001$ versus the combination. rhIGFBP, Recombinant human insulin-like growth factor-binding protein 3; NF-κB, nuclear factor kappa B.

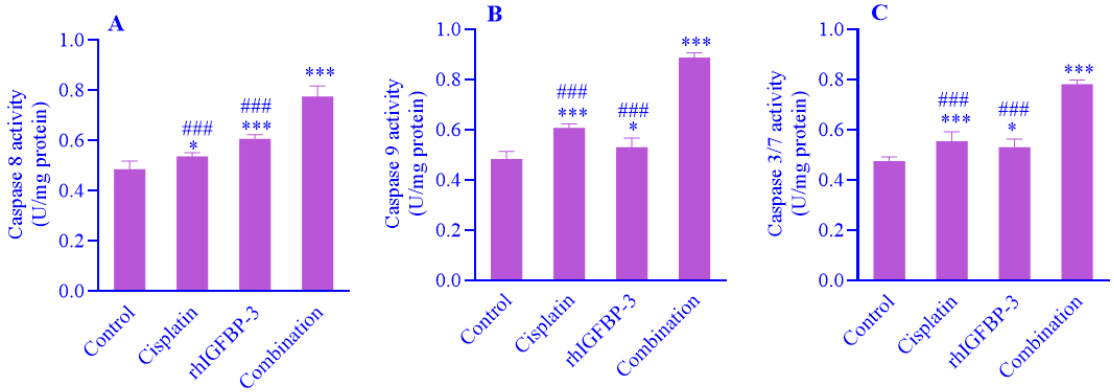

Fig. 7. The effect of cisplatin, rhIGFBP-3, and their combination on caspase activity. Data are expressed as mean ± SD (n = 9). *$P \leq 0.05$, **$P \leq 0.01$, and ***$P \leq 0.001$ indicate significant differences in comparison with the control group; $^{\#\#\#}P \leq 0.001$ versus the combination. rhIGFBP, Recombinant human insulin-like growth factor-binding protein 3;

Regulation of NF-κB downstream target gene expression by cisplatin, rhIGFBP-3, and their combination

We examined the mRNA expression levels of BAX and BCL-2 to assess the potential of cisplatin, rhIGFBP-3, or their combination, at the indicated concentration and duration, to activate apoptosis. Furthermore, we analyzed the expression of inflammation-related genes (IL-6, IL-8, iNOS, and COX-2), which are downstream targets of NF-κB and influence the balance between programmed cell death and cell survival. This assessment was done to clarify how these pro-inflammatory factors affect apoptotic and survival signaling pathways in our target cells. Statistical analysis revealed that, compared to the control group, both cisplatin and rhIGFBP-3 markedly upregulated BAX expression. Moreover, the combination of both treatments led to a noticeably greater increase in BAX expression than either treatment alone (Fig. 8A). All three treatment groups led to a notable downregulation of BCL-2 levels compared to the untreated control group. Additionally, the combination group decreased BCL-2 levels compared to cisplatin alone and more substantially than rhIGFBP-3 alone (Fig. 8B). Relative to the control group, the BAX/BCL-2 ratio increased markedly in all three treatment groups. Furthermore, the combination treatment produced a significantly greater increase in the ratio compared to the individual treatments (Fig. 8C). Regarding the expression of genes implicated in inflammatory regulation, it was found that cisplatin markedly elevated the levels of IL-6, IL-8, COX-2, and iNOS compared to the untreated control group. In contrast, rhIGFBP-3 treatment led to a notable reduction in all these inflammation-promoting factors. Interestingly, the combination group exhibited a significant decrease in IL-6, IL-8, COX-2, and iNOS compared to cisplatin treatment alone. However, when compared to the control group, COX-2 and iNOS levels remained significantly elevated, while IL-6 and IL-8 showed a slight, non-significant increase. Furthermore, the combination group displayed significantly higher expression in IL-6, IL-8, COX-2, and iNOS levels relative to the rhIGFBP-3 group (Fig. 8D-F).

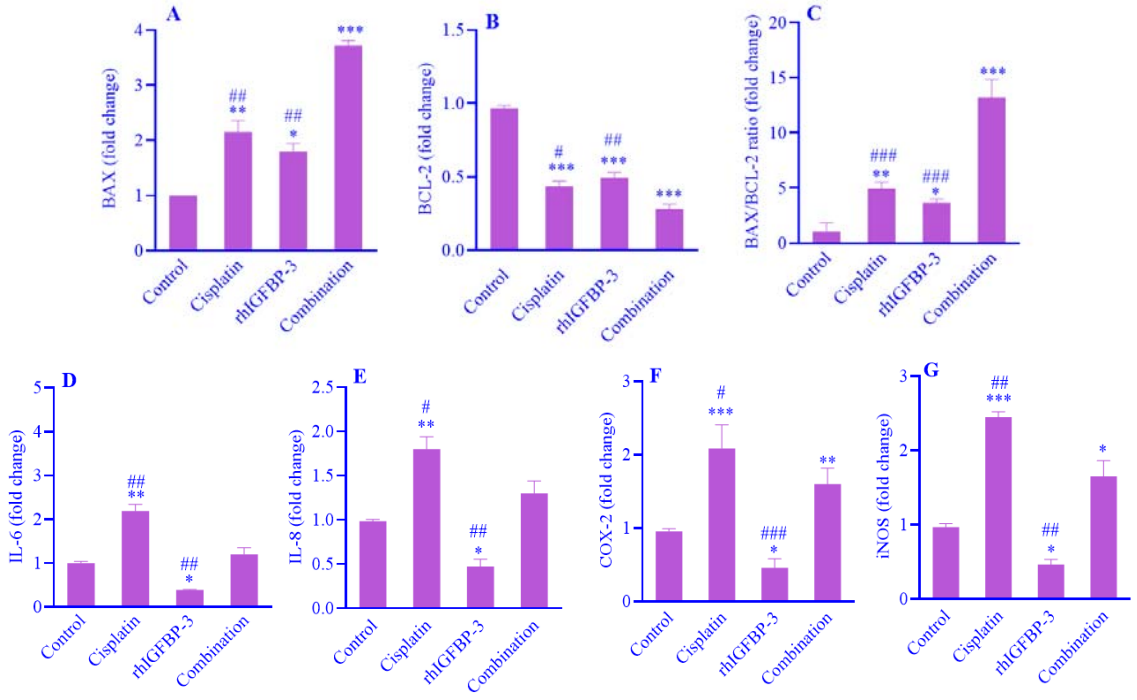

Fig. 8. Impact of cisplatin, rhIGFBP-3, and their combination on the expression of apoptosis- and inflammation-associated genes in HeLa cells. The cells were treated with the specified concentration and duration in three separate tests, each done in triplicate. The data are presented as mean ± SD. $^{*}P \leq 0.05$, $^{**}P \leq 0.01$, and $^{***}P \leq 0.001$ indicate significant differences in comparison with the control group; $^{\#}P \leq 0.05$, $^{\#\#}P \leq 0.01$, $^{\#\#\#}P \leq 0.001$ versus the combination. rhIGFBP, Recombinant human insulin-like growth factor-binding protein 3; Bcl-2, B-cell lymphoma 2; BAX, Bcl-2-associated X protein; IL, interleukin; COX, cyclooxygenase; iNOS, inducible nitric oxide synthase.

DISCUSSION

CC involves complex molecular and cellular pathways, making it a lasting obstacle in healthcare (6). Its onset is influenced by the continuous deregulation of multiple inflammatory pathways, with NF-κB playing a central role. HPV 16+ and HPV 18+ are frequently linked to the activation of NF-κB in CC (27), a process that is further intensified by cisplatin treatment and ultimately contributes to therapy resistance (28). Identifying new treatment modalities remains essential in light of these challenges. Growing evidence supports that combination therapies can minimize treatment-related toxicity while improving treatment effectiveness (29). This study presents evidence for the benefits of combining cisplatin with an NF-κB inhibitor to improve treatment outcomes and reduce the required dosage of cisplatin.

This research represented the first investigation into the dual function of IGFBP-3 as both a potentiator of cisplatin-induced apoptosis and an inhibitor of NF-κB in HeLa cells. We explored whether IGFBP-3's pro-apoptotic effects were related to its regulation of inflammatory processes. Using the MTT assay, we assessed IGFBP-3's impact on cell viability. Cell death mechanisms were identified through cell cycle analysis, the TUNEL assay, and annexin V/PI labeling. The molecular mechanisms of apoptosis were verified by measuring caspase activities and evaluating the Bax/Bcl-2 ratio. To scrutinize the relationship between apoptosis and inflammation, we analyzed NF-κB p65 protein levels by western blot and quantified pro-inflammatory transcripts using real-time PCR. Extensive research has highlighted the multifaceted functions of IGFBP-3 in cancer, as it can act as either an oncogenic driver or a tumor suppressor, depending on the specific biological context. Numerous studies have shown that IGFBP-3 induces apoptosis across a range of malignancies, including prostate, breast, esophageal, osteosarcoma, lung, and oral cancers. This pro-apoptotic activity may occur through elevated ectopic expression, administration as an exogenous protein, or synergistically with radiotherapy and chemotherapy (19,30-35). However, in some cancers, such as squamous cell carcinomas (cutaneous and of the tongue), glioblastoma, and triple-negative breast cancer, elevated IGFBP-3 levels have been associated with increased cancer cell survival or reduced therapeutic efficacy (36-39). The MTT results of the current study indicated that rhIGFBP-3 aided in suppressing HeLa cell growth when used in combination with cisplatin. Both agents exhibited a concentration-dependent reduction in cell viability. CI analysis validated the synergistic anticancer effects (CI < 1), suggesting that a lower cisplatin concentration could be effective when used with rhIGFBP-3. The DRI further highlighted the therapeutic potential of this combination therapy.

To offer reliable data on the suppression of cell growth, we used annexin V/PI and TUNEL staining methods to assess early and late apoptosis and DNA fragmentation, respectively. Compared to therapy alone or no treatment, analysis of the annexin V/PI assay showed that rhIGFBP-3 combined with cisplatin dramatically exacerbated total apoptosis in HeLa cells. This clearly elucidated the pro-apoptotic roles of IGFBP-3 in cancer. Additionally, TUNEL assay results corroborated previous findings and indicated that the combination of cisplatin and rhIGFBP-3 significantly enhanced DNA fragmentation in HeLa cells compared to either treatment alone, with evidence of apoptosis obtained from the annexin V/PI assay corresponding accordingly. Previous research has shown that ectopic expression of IGFBP-3 occurs in radiation-exposed oral squamous cell carcinoma, suggesting that ionization increases the rate of apoptosis evident through annexin V/PI staining and resultant DNA fragmentation *in vivo* (35). According to findings of the research conducted by Williams *et al*., secretory or synthetic IGFBP-3 can elevate apoptosis by up to 30% in colon carcinoma cells *via* induction of tumor necrosis factor (TNF)-related apoptosis-inducing ligand (TRAIL), while not affecting TRAIL-resistant or non-tumor cells (40). Another study confirmed that increased IGFBP-3 gene expression causes DNA damage in microglia while protecting neurons during ischemic events (41). Recently, Wen *et al.* reported that doxorubicin-treated cardiomyocytes exhibited elevated intracellular and secreted IGFBP-3 levels. This elevation subsequently disrupted IGF1-mediated survival signaling and led to a

significant increase in TUNEL-positive cardiomyocytes (42). Contrary to our findings, a study on cutaneous epidermoid carcinoma revealed that knockdown of the IGFBP-3 gene significantly increased DNA fragmentation (36).

Following the above methods, we examined the cell cycle distribution to scrutinize how our therapies targeted the cell cycle to prevent HeLa cell growth. Investigations have highlighted that IGFBP-3 is indispensable for managing cell cycle arrest and provoking apoptosis in various cancers. Wu *et al.* identified that IGFBP-3 drove G1/S phase arrest and cell death in a variety of breast malignancy cell lines (43), while Peng *et al.* concluded that IGFBP-3 contributed to G1 phase arrest in lymph node carcinoma of the prostate cells and enabled cell growth suppression by high doses of androgens (44). In agreement with these findings, O'Han *et al.* revealed that IGFBP-3 knockdown in human breast cancer cells facilitated cell cycle progression from G0/G1 to the S phase, enhancing cell growth (45). Similarly, esophageal squamous cell carcinoma cells with increased IGFBP-3 expression exhibited G1/S phase arrest and demonstrated enhanced sensitivity to radiation (46), whereas Wang *et al.* documented G2/M accumulation upon irradiation in human oral epidermoid carcinoma cells with p53 mutations (35). In contrast to cisplatin alone, rhIGFBP-3 therapy in our study resulted in a considerable G1 phase arrest, while the sub-G1 population, indicating apoptosis, was smaller. However, co-treatment with rhIGFBP-3 and cisplatin caused a meaningful enhancement in the sub-G1 population, reflecting increased apoptosis and a decline in S-phase cells. These findings support the idea that, depending on the context and cell type, IGFBP-3 triggers apoptosis and cell cycle arrest.

We clarified the molecular mechanisms of apoptosis in response to treatments by examining the expression levels of the BAX and BCL-2 genes, along with the activity of caspases 8, 9, and 3/7. Our findings emphasized an increase in the activity of caspases 8, 9, and 3/7 and demonstrated an elevated BAX/BCL-2 ratio following rhIGFBP-3 treatment, both alone and in combination with cisplatin. Based on these analyses, rhIGFBP-3 treatment initiated both intrinsic and extrinsic mitochondrial apoptotic pathways. These observations supported earlier findings in cancer and pancreatic beta cells, indicating that IGFBP-3 triggered the extrinsic mitochondrial pathway by activating caspase-8 through its death receptor TMEM219, which in turn initiated the intrinsic apoptotic pathway (47-49). The observed suppression of BCL-2 and upregulation of BAX, culminating in enhanced apoptosis with caspases 3/7 functioning as the final executioners of programmed cell death, further reinforced this mechanism. These results aligned with the findings of Agostini-Dreyer and colleagues, demonstrating that exogenous IGFBP-3 accelerated the nuclear entry of nuclear receptor subfamily 4 group A member 1, thereby promoting intrinsic apoptosis (50). Moreover, Buttet *et al.* validated that ectopic IGFBP-3 expression, achieved through cDNA transfection in breast cancer cells, modulated the transcription of Bax and BCL-2, both individually and in response to ionizing radiation (31). In line with these findings, we previously reported that the rhIGFBP-3/TMEM219 axis in resistant pancreatic ductal adenocarcinoma cells enhanced Bax expression, suppressed BCL-2, and activated caspases 8 and 3, ultimately leading to intrinsic apoptosis (16).

NF-κB is widely recognized as a key survival factor in cancer, playing a significant role in cancer progression by activating anti-apoptotic genes such as BCL-2, B-cell lymphoma-extra-large, and inhibitor of apoptosis proteins, as well as pro-inflammatory genes like IL-6, IL-8, iNOS, and COX-2 (51,52). The dysregulation of these genes fosters a tumor-promoting environment by enhancing cancer cell proliferation, promoting resistance to apoptosis, and reducing the effectiveness of anticancer therapies (53-55). NF-κB activation is classically mediated by the canonical pathway, where stimuli such as cytokines, pathogens, or stress signals trigger inhibitor of kappa B (IκB) kinase (IKK)-dependent phosphorylation and subsequent degradation of IκBα, releasing NF-κB (primarily p65/p50 heterodimers) for nuclear translocation and transcriptional activation of target genes. Numerous studies have reported that inhibiting NF-κB can induce apoptosis in tumor cells or increase their sensitivity to therapeutic agents (56,57). In addition, IGFBP-3-mediated inhibition of NF-κB has been implicated in multiple diseases (21-25,40). Notably, IGFBP-3

can suppress NF-κB through caspase-dependent degradation of total p65, unlike conventional IKK inhibitors that solely block phosphorylation without affecting total protein levels (24). Our observations prompted a critical question regarding the mechanism of rhIGFBP-3 action: were the observed apoptotic and cisplatin-sensitizing effects in HeLa cells a consequence of its anti-inflammatory properties? To investigate this, we quantified NF-kB p65 protein levels by western blotting and assessed the expression of its downstream inflammatory target genes using RT-PCR. Our findings corresponded with our initial theoretical foundations and reflected previous studies. rhIGFBP-3 significantly decreased the level of NF-kB p65 protein and led to a statistically significant reduction in the expression of its downstream inflammatory genes compared to the control group. In combination with cisplatin, rhIGFBP-3 also significantly reduced NF-κB p65 protein levels and resulted in a statistically significant downregulation of the expression of its downstream inflammatory genes compared to the cisplatin-treated group. The findings of the study conducted by Kang *et al.,* consistent with our results, showed that rhIGFBP-3 mitigated lipopolysaccharide-induced acute lung injury in mice by inhibiting the expression of NF-κB and pro-inflammatory cytokines, including TNFα, IL-6, IL-1β, and interferon-gamma in lung tissues (58). In a study using human hepatocellular carcinoma, overexpression of IGFBP-3 inhibited NF-κB activity and reduced IL-8 secretion stimulated by palmitate (25). Another *in vitro* study using an adenovirus vector expressing IGFBP-3 in human osteoarthritis-like fibroblast synoviocytes documented that IGFBP-3 suppressed inflammation by inhibiting NF-κB activation and TNFα-induced chemokine secretion, while also sensitizing the cells to TNFα-induced apoptosis (59). Likewise, Bogdan *et al*. showed that rhIGFBP-3 mediated hyperosmolar inflammation, a key factor in dry eye pathogenesis, by partially reducing IL-8 levels in human telomerase-immortalized corneal epithelial cells (60). Conversely, another study reported that ectopic IGFBP-3 expression increased ionizing radiation-induced oral squamous cell carcinoma cell death by activating NF-κB, triggering cytokine expression, and promoting the production of reactive oxygen species (35). These findings from our study, along with previous research, suggested that IGFBP-3 played an anti-inflammatory role by modulating NF-κB signaling. However, its effects may differ based on the tissue type and the specific disease context.

Collectively, our *in vitro* findings indicated that rhIGFBP-3, either as a monotherapy or in combination with cisplatin, downregulated NF-κB p65 and its downstream inflammation-related genes, modulated cell survival and apoptotic signaling pathways, and induced cell cycle arrest in HeLa cells, thereby exhibiting significant antitumor activity. These mechanistic results suggested the therapeutic potential of rhIGFBP-3, particularly its ability to enhance cisplatin cytotoxicity at reduced concentrations. However, we emphasize that direct evidence for reduced chemotherapy-induced side effects requires comprehensive *in vivo* toxicity studies, which were beyond the scope of the current investigation.

CONCLUSION

rhIGFBP-3, either alone or in combination with cisplatin, functioned as a tumor suppressor in HPV18-infected HeLa cells. It showed potential anticancer effects in HPV18-related CC cells by inhibiting cell proliferation, inducing cell cycle arrest, and modulating inflammatory factors, likely through the suppression of NF-κB signaling. Our findings suggest that rhIGFBP-3 lowers NF-kB p65 total levels and amplifies cisplatin's cytotoxic effects, potentially allowing for lower doses of the drug, which could be a promising target for treating HPV18-related CC. However, additional *in vivo* and *in vitro* research is required to fully understand the mechanisms through which rhIGFBP-3 leads to inactivation of the NF-κB pathway, cell death, and reduction of chemotherapy side effects.

Limitation

We acknowledge that the exclusive use of HeLa cells and the absence of *in vivo* or clinical data represent important limitations that constrain the broader applicability of these findings. Future studies should validate these observations in additional NF-κB-dependent cancer models and, crucially, incorporate preclinical animal studies to evaluate both therapeutic efficacy and potential toxicity reduction. Such investigations will be

essential to establish the translational relevance of rhIGFBP-3 and explore its interactions within the tumor microenvironment and inflammatory responses.

Acknowledgements

This work was financially supported by the Vice-Chancellery of Research of the Isfahan University of Medical Sciences through Grant No. 3401688.

Conflict of interest statement

All authors declared no conflict of interest in this study.

Authors' contributions

H. Arab was involved in the conceptualization, investigation, and methodology of the study, and took the lead in writing the original draft and participating in the review and editing process. M. Shokrzadeh oversaw methodology development and was responsible for supervision and project administration throughout the study. T. Mousavi participated in methodological work and assisted with the review and editing of the manuscript. M.R. Mofid played a key role in conceptualization and investigation, provided supervision and project administration, and was engaged in reviewing and editing the manuscript. All authors have read and approved the finalized article. Each author has fulfilled the authorship criteria and affirmed that this article represents honest and original work.

AI declaration

The authors used QuillBot to paraphrase and improve grammatical and verb consistency in certain sections during the preparation of this work. All content was thoroughly reviewed, and the authors acknowledge full accountability for the integrity and accuracy of the publication.

Data availability

All data obtained from the analysis of this work are documented and available upon reasonable request directed to the corresponding author.

REFERENCES

1. Jallah JK, Anjankar A, Nankong FA. Public health approach in the elimination and control of cervical cancer: a review. Cureus. 2023;15(9):1-9. DOI: 10.7759/cureus.44543.
2. Burmeister CA, Khan SF, Schäfer G, Mbatani N, Adams T, Moodley J, *et al*. Cervical cancer therapies: current challenges and future perspectives. Tumour Virus Res. 2022;13:200238,1-14. DOI: 10.1016/j.tvr.2022.200238.
3. Romani AM. Cisplatin in cancer treatment. Biochem Pharmacol. 2022;206:115323. DOI: 10.1016/j.bcp.2022.115323.
4. Bhattacharjee R, Dey T, Kumar L, Kar S, Sarkar R, Ghorai M, *et al*. Cellular landscaping of cisplatin resistance in cervical cancer. Biomed Pharmacother. 2022;153:113345. DOI: 10.1016/j.biopha.2022.113345.
5. Vitkauskaite A, Urboniene D, Celiesiute J, Jariene K, Skrodeniene E, Nadisauskiene RJ, *et al*. Circulating inflammatory markers in cervical cancer patients and healthy controls. J Immunotoxicol. 2020;17(1): 105-109. DOI: 10.1080/1547691X.2020.1755397.
6. Revathidevi S, Murugan AK, Nakaoka H, Inoue I, Munirajan AK. APOBEC: a molecular driver in cervical cancer pathogenesis. Cancer Lett. 2021;496:104-116. DOI: 10.1016/j.canlet.2020.10.004.
7. Fernandes JV, de Medeiros Fernandes TAA, de Azevedo JCV, Cobucci RNO, de Carvalho MGF, Andrade VS, *et al*. Link between chronic inflammation and human papillomavirus-induced carcinogenesis. Oncol Lett. 2015;9(3):1015-1026. DOI: 10.3892/ol.2015.2884.
8. Deng S, Yuan P, Sun J. The role of NF-κB in carcinogenesis of cervical cancer: opportunities and challenges. Mol Biol Rep. 2024;51(1):538. DOI: 10.1007/s11033-024-09447-z.
9. Godwin P, Baird AM, Heavey S, Barr M, O'Byrne K, Gately K. Targeting nuclear factor-kappa B to overcome resistance to chemotherapy. Front Oncol. 2013;3: 120,1-10. DOI: 10.3389/fonc.2013.00120.
10. Hemmat N, Bannazadeh Baghi H. Association of human papillomavirus infection and inflammation in cervical cancer. Pathog Dis. 2019;77(5):ftz048,1-11. DOI: 10.1093/femspd/ftz048.
11. da Costa RMG, Bastos MM, Medeiros R, Oliveira PA. The NFκB signaling pathway in papillomavirus-induced lesions: friend or foe? Anticancer Res. 2016;36(5): 2073-2083. PMID: 27127107.
12. Hernandez-Flores G, Ortiz-Lazareno P, Lerma-Diaz J, Dominguez-Rodriguez J, Jave-Suarez L, Bravo-Cuellar A. Pentoxifylline sensitizes human cervical tumor cells to cisplatin-induced apoptosis by suppressing NF-κB and decreased cell senescence. BMC Cancer. 2011;11(1):483,1-15. DOI: 10.1186/1471-2407-11-483.
13. Garcia-Becerra N, Aguilar-Lemarroy A, Jave-Suarez LF. On the regulation of NF-κB pathway by HPV oncoproteins: are pathway inhibitors a good alternative for the treatment of cervical cancer? Anticancer Agents Med Chem. 2023;23(5):492-497. DOI: 10.2174/1871520622666220509180606.
14. Ansari A, Gheysarzadeh A, Sharifi A, Mofid MR. Clinicopathological correlation of insulin-like growth

factor binding protein 3 and their death receptor in patients with gastric cancer. Res Pharm Sci. 2024;19(1):42-52. DOI: 10.4103/1735-5362.394819.
15. Yan J, Yang X, Li L, Liu P, Wu H, Liu Z, *et al*. Low expression levels of insulin-like growth factor binding protein-3 are correlated with poor prognosis for patients with hepatocellular carcinoma. Oncol Lett. 2017;13(5):3395-3402. DOI: 10.3892/ol.2017.5934.
16. Mofid MR, Gheysarzadeh A, Bakhtiyari S. Insulin-like growth factor binding protein 3 chemosensitizes pancreatic ductal adenocarcinoma through its death receptor. Pancreatology. 2020;20(7): 1442-1450. DOI: 10.1016/j.pan.2020.07.406.
17. Sharma M, Satyam A, Abhishek A, Khan R, Rajappa M, Sharma A. Molecular and circulatory expression of insulin growth factors in Indian females with advanced cervical cancer. Asian Pac J Cancer Prev. 2012;13(12):6475-6479. DOI: 10.7314/apjcp.2012.13.12.6475.
18. Mehta HH, Gao Q, Galet C, Paharkova V, Wan J, Said J, *et al*. IGFBP-3 is a metastasis suppression gene in prostate cancer. Cancer Res. 2011;71(15):5154-5163. DOI: 10.1158/0008-5472.CAN-10-4513.
19. Wang YA, Sun Y, Palmer J, Solomides C, Huang LC, Shyr Y, *et al*. IGFBP-3 modulates lung tumorigenesis and cell growth through IGF1 signaling. Mol Cancer Res. 2017;15(7):896-904. DOI: 10.1158/1541-7786.MCR-16-0390.
20. Li C, Harada A, Oh Y. IGFBP-3 sensitizes antiestrogen-resistant breast cancer cells through interaction with GRP78. Cancer Lett. 2012;325(2):200-206. DOI: 10.1016/j.canlet.2012.07.004.
21. Han J, Jogie-Brahim S, Harada A, Oh Y. Insulin-like growth factor-binding protein-3 suppresses tumor growth *via* activation of caspase-dependent apoptosis and cross-talk with NF-κB signaling. Cancer Lett. 2011;307(2):200-210. DOI: 10.1016/j.canlet.2011.04.004.
22. Mohanraj L, Kim HS, Li W, Cai Q, Kim KE, Shin HJ, *et al*. IGFBP-3 inhibits cytokine-induced insulin resistance and early manifestations of atherosclerosis. PLoS One. 2013;8(1):e55084,1-13. DOI: 10.1371/journal.pone.0055084
23. Lee HS, Woo SJ, Koh HW, Ka SO, Zhou L, Jang KY, *et al*. Regulation of apoptosis and inflammatory responses by insulin-like growth factor binding protein 3 in fibroblast-like synoviocytes and experimental animal models of rheumatoid arthritis. Arthritis Rheumatol. 2014;66(4):863-873. DOI: 10.1002/art.38303.
24. Lee YC, Jogie-Brahim S, Lee DY, Han J, Harada A, Murphy LJ, *et al*. Insulin-like growth factor-binding protein-3 (IGFBP-3) blocks the effects of asthma by negatively regulating NF-κB signaling through IGFBP-3R-mediated activation of caspases. J Biol Chem. 2011;286(20):17898-17909. DOI: 10.1074/jbc.M111.231035.
25. Min HK, Maruyama H, Jang BK, Shimada M, Mirshahi F, Ren S, *et al*. Suppression of IGF binding protein-3 by palmitate promotes hepatic inflammatory responses. FASEB J. 2016;30(12):4071-4082. DOI: 10.1096/fj.201600427R.
26. Chou TC, Talalay P. Quantitative analysis of dose-effect relationships: the combined effects of multiple drugs or enzyme inhibitors. Adv Enzyme Regul. 1984;22:27-55. DOI: 10.1016/0065-2571(84)90007-4.
27. Pasha A, Kumar K, Heena S, Arnold Emerson I, Pawar SC. Inhibition of NF-κB and COX-2 by andrographolide regulates the progression of cervical cancer by promoting PTEN expression and suppressing PI3K/AKT signaling pathway. Sci Rep. 2024;14(1):12020,1-22. DOI: 10.1038/s41598-024-57304-7.
28. Sarwar S, Yu JQ, Nadeem H, Huq F. Synergistic cytotoxic effect from combination of wedelolactone and cisplatin in HeLa cell line: a novel finding. Drug Des Devel Ther. 2020;14:3841-3852. DOI: 10.2147/DDDT.S261321.
29. Bhatia K, Das A. Combinatorial drug therapy in cancer: new insights. Life Sci. 2020;258:118134,1-27. DOI: 10.1016/j.lfs.2020.118134.
30. Massoner P, Colleselli D, Matscheski A, Pircher H, Geley S, Dürr PJ, *et al*. Novel mechanism of IGF-binding protein-3 action on prostate cancer cells: inhibition of proliferation, adhesion, and motility. Endocr Relat Cancer. 2009;16(3):795-808. DOI: 10.1677/ERC-08-0175.
31. Butt AJ, Firth SM, King MA, Baxter RC. Insulin-like growth factor-binding protein-3 modulates expression of Bax and Bcl-2 and potentiates p53-independent radiation-induced apoptosis in human breast cancer cells. J Biol Chem. 2000;275(50):39174-39181. DOI: 10.1074/jbc.M908888199.
32. Luo LL, Zhao L, Xi M, He LR, Shen JX, Li QQ, *et al*. Association of insulin-like growth factor-binding protein-3 with radiotherapy response and prognosis of esophageal squamous cell carcinoma. Cancer Commun. 2015;34(11):514-521. DOI: 10.1186/s40880-015-0046-2.
33. Schedlich LJ, Yenson VM, Baxter RC. TGF-β-induced expression of IGFBP-3 regulates IGF1R signaling in human osteosarcoma cells. Mol Cell Endocrinol. 2013;377(1-2):56-64. DOI: 10.1016/j.mce.2013.06.033.
34. Lin M, Marzec K, Martin J, Baxter R. The role of insulin-like growth factor binding protein-3 in the breast cancer cell response to DNA-damaging agents. Oncogene. 2014;33(1):85-96. DOI: 10.1038/onc.2012.538.
35. Wang SH, Chen YL, Hsiao JR, Tsai FY, Jiang SS, Lee AYL, *et al*. Insulin-like growth factor binding protein 3 promotes radiosensitivity of oral squamous cell carcinoma cells *via* positive feedback on NF-κB/IL-6/ROS signaling. J Exp Clin Cancer Res. 2021;40(1):95,1-18. DOI: 10.1186/s13046-021-01898-7.
36. Liu J, Guo Y, Huang Y, Xue H, Bai S, Zhu J, *et al*. Effects of insulin-like growth factor binding protein 3 on apoptosis of cutaneous squamous cell carcinoma cells. Onco Targets Ther. 2018;11:6569-6577. DOI: 10.2147/OTT.S167187.
37. Ng EFY, Kaida A, Nojima H, Miura M. Roles of IGFBP-3 in cell migration and growth in an endophytic tongue squamous cell carcinoma cell line. Sci Rep. 2022;12(1):11503,1-14.

DOI: 10.1038/s41598-022-15737-y.
38. Thota B, Arimappamagan A, Kandavel T, Shastry AH, Pandey P, Chandramouli BA, *et al*. STAT-1 expression is regulated by IGFBP-3 in malignant glioma cells and is a strong predictor of poor survival in patients with glioblastoma. J Neurosurg. 2014;121(2):374-383. DOI: 10.3171/2014.4.JNS131198.
39. Chen CH, Chen PY, Lin YY, Feng LY, Chen SH, Chen CY, *et al*. Suppression of tumor growth *via* IGFBP3 depletion as a potential treatment in glioma. J Neurosurg. 2019;132(1):168-179. DOI: 10.3171/2018.8.JNS181217.
40. Williams AC, Smartt H, Macfarlane M, Paraskeva C, Collard T. Insulin-like growth factor binding protein 3 (IGFBP-3) potentiates TRAIL-induced apoptosis of human colorectal carcinoma cells through inhibition of NF-κB. Cell Death Differ. 2007;14(1):137-145. DOI: 10.1038/sj.cdd.4401919.
41. Kielczewski JL, Hu P, Shaw LC, Calzi SL, Mames RN, Gardiner TA, *et al*. Novel protective properties of IGFBP-3 result in enhanced pericyte ensheathment, reduced microglial activation, increased microglial apoptosis, and neuronal protection after ischemic retinal injury. Am J Pathol. 2011;178(4):1517-1528. DOI: 10.1016/j.ajpath.2010.12.031.
42. Wen SY, Ali A, Huang IC, Liu JS, Chen PY, Viswanadha VP, *et al*. Doxorubicin-induced ROS-dependent HIF1α activation mediates blockage of IGF1R survival signaling by IGFBP3 promotes cardiac apoptosis. Aging (Albany). 2023;15(1):164-178. DOI: 10.18632/aging. 204466.
43. Wu C, Liu X, Wang Y, Tian H, Xie Y, Li Q, *et al*. Insulin-like growth factor binding protein-3 promotes the G1 cell cycle arrest in several cancer cell lines. Gene. 2013;512(1):127-133. DOI: 10.1016/j.gene.2012.09.080.
44. Peng L, Wang J, Malloy PJ, Feldman D. The role of insulin-like growth factor binding protein-3 in the growth inhibitory actions of androgens in LNCaP human prostate cancer cells. Int J Cancer. 2008;122(3):558-566. DOI: 10.1002/ijc.23100.
45. O'Han MK, Baxter RC, Schedlich LJ. Effects of endogenous insulin-like growth factor binding protein-3 on cell cycle regulation in breast cancer cells. Growth Factors. 2009;27(6):394-408. DOI: 10.3109/08977190903185032.
46. Luo L, Zhao L, Wang Y, Tian X, Xi M, Shen J, *et al*. Insulin-like growth factor binding protein-3 is a new predictor of radiosensitivity on esophageal squamous cell carcinoma. Sci Rep. 2015;5:17336,1-12. DOI: 10.1038/srep17336.
47. Ingermann AR, Yang YF, Han J, Mikami A, Garza AE, Mohanraj L, *et al*. Identification of a novel cell death receptor mediating IGFBP-3-induced anti-tumor effects in breast and prostate cancer. J Biol Chem. 2010;285(39):30233-30246. DOI: 10.1074/jbc.M110.122226.
48. Kim HS, Ingermann AR, Tsubaki J, Twigg SM, Walker GE, Oh Y. Insulin-like growth factor-binding protein 3 induces caspase-dependent apoptosis through a death receptor-mediated pathway in MCF-7 human breast cancer cells. Cancer Res. 2004;64(6):2229-2237. DOI: 10.1158/0008-5472.can-03-1675.
49. D'Addio F, Maestroni A, Assi E, Ben Nasr M, Amabile G, Usuelli V, *et al*. The IGFBP3/TMEM219 pathway regulates beta cell homeostasis. Nat Commun. 2022;13(1):684,1-14. DOI: 10.1038/s41467-022-28360-2.
50. Agostini-Dreyer A, Jetzt AE, Stires H, Cohick WS. Endogenous IGFBP-3 mediates intrinsic apoptosis through modulation of Nur77 phosphorylation and nuclear export. Endocrinology. 2015;156(11):4141-4151. DOI: 10.1210/en.2015-1215.
51. Puar YR, Shanmugam MK, Fan L, Arfuso F, Sethi G, Tergaonkar V. Evidence for the involvement of the master transcription factor NF-κB in cancer initiation and progression. Biomedicines. 2018;6(3): 82,1-21. DOI: 10.3390/biomedicines6030082.
52. Moawadh MS, Mir R, Tayeb FJ, Asim O, Ullah MF. Molecular evaluation of the impact of polymorphic variants in apoptotic (Bcl-2/Bax) and proinflammatory cytokine (TNF-α/IL-8) genes on the susceptibility and progression of myeloproliferative neoplasms:a case-control biomarker study. Curr Issues Mol Biol. 2023;45(5):3933-3952. DOI: 10.3390/cimb45050251.
53. Shah A, Patel C. A concise review of inflammatory biomarkers targeted cancer therapy. Folia Med (Plovdiv). 2022;64(4):572-580. DOI: 10.3897/folmed.64.e68365.
54. Hafezi S, Rahmani M. Targeting BCL-2 in cancer: advances, challenges, and perspectives. Cancers (Basel). 2021;13(6):1292,1-15. DOI: 10.3390/cancers13061292.
55. Pogmore JP, Uehling D, Andrews DW. Pharmacological targeting of executioner proteins: controlling life and death. J Med Chem. 2021;64(9):5276-5290. DOI: 10.1021/acs.jmedchem.0c02200.
56. Wu X, Sun L, Xu F. NF-κB in cell deaths, therapeutic resistance and nanotherapy of tumors: recent advances. Pharmaceuticals (Basel). 2023;16(6):783,1-22. DOI: 10.3390/ph16060783.
57. Akbarpour Arsanjani A, Abuei H, Behzad-Behbahani A, Bagheri Z, Arabsolghar R, Farhadi A. Activating transcription factor 3 inhibits NF-κB p65 signaling pathway and mediates apoptosis and cell cycle arrest in cervical cancer cells. Infect Agent Cancer. 2022;17(1):62,1-10. DOI: 10.1186/s13027-022-00475-7.
58. Kang L, Li X, Liu J, Li Y, Li S, Zhao C. Recombinant human insulin-like growth factor binding protein 3 attenuates lipopolysaccharide-induced acute lung injury in mice. Int J Clin Exp Pathol. 2020;13(7): 1924-1931. PMID: 32782724.
59. Zhang XL, Li HH, Cao YP, Peng F, Li JP. Insulin-like growth factor binding protein 3 inhibits inflammatory response and promotes apoptosis in fibroblast-like synoviocytes of osteoarthritis. Int J Clin Exp Pathol. 2017;10:3024-3032.
60. Bogdan ED, Stuard WL, Titone R, Robertson DM. IGFBP-3 mediates metabolic homeostasis during hyperosmolar stress in the corneal epithelium. Invest Ophthalmol Vis Sci. 2021;62(7):11,1-11. DOI: 10.1167/iovs.62.7.11.